

# Generation of dark-bright soliton trains in superfluid-superfluid counterflow

C. Hamner, J.J. Chang, and P. Engels\*

*Washington State University, Department of Physics and Astronomy, Pullman, Washington 99164, USA*

M. A. Hofer

*North Carolina State University, Department of Mathematics, Raleigh, NC 27695, USA*

The dynamics of two penetrating superfluids exhibit an intriguing variety of nonlinear effects. Using two distinguishable components of a Bose-Einstein condensate, we investigate the counterflow of two superfluids in a narrow channel. We present the first experimental observation of trains of dark-bright solitons generated by the counterflow. Our observations are theoretically interpreted by three-dimensional numerical simulations for the coupled Gross-Pitaevskii (GP) equations and the analysis of a jump in the two relatively flowing components' densities. Counterflow induced modulational instability for this miscible system is identified as the central process in the dynamics.

PACS numbers: 03.75.Kk, 67.85.De, 47.40.x, 05.45.Yv

Nonlinear structures in dilute-gas Bose-Einstein condensates (BECs) have been the focus of intense research efforts, deepening our understanding of quantum dynamics and providing intriguing parallels between atomic physics, condensed matter and optical systems. For superfluids that are confined in a narrow channel, one of the most prominent phenomena of nonlinear behavior is the existence of solitons in which a tendency to disperse is counterbalanced by the nonlinearities of the system. In single-component BECs, dark and bright solitons, forming local density suppressions and local bumps in the density, resp., have attracted great interest [1]. In two-component BECs, the dynamics are even richer as a new degree of freedom, the relative flow between the two components, is possible.

In this Letter, we investigate novel dynamics of superfluid-superfluid counterflow, which is in contrast to the extensively studied counterflow of a superfluid and normal fluid in liquid helium [2]. Previous theoretical analysis has demonstrated that spatially uniform, counterflowing superfluids exhibit modulational instability (MI) when the relative speed exceeds a critical value [3]. Modulational instability is characterized by a rapid growth of long wavelength, small amplitude perturbations to a carrier wave into large amplitude modulations. The growth is due to the nonlinearity in the system [4]. Our experiments and analysis reveal that by carefully tuning the relative speed slightly above the critical value, we can enhance large amplitude density modulations at the overlap interface between two nonlinearly coupled BEC components while mitigating the effects of MI in the slowly varying background regions. A dark-bright soliton train then results.

In two previous experiments, individual dark-bright solitons were engineered in two stationary components using a wavefunction engineering technique [5, 6]. In our experiment we find that trains of dark-bright solitons can occur quite naturally in superfluid counterflow. This novel method of generating dark-bright solitons turns

out to be robust and repeatable. In single-component, attractive BECs the formation of a bright soliton train from an initial density jump has been predicted [7]. However, both condensate collapse and the effects of MI in the density background must be avoided, placing restrictions on the confinement geometry and diluteness of the single-component condensate. In contrast, the properties of counterflow in miscible, two-component BECs, as we show, enable the observation of trains consisting of ten or more dark-bright solitons in BECs with a large number of atoms. We also note that modulated soliton trains have been studied extensively in single-component, modulationally stable repulsive BECs where supersonic flow supports the generation of dispersive shock waves [8]. The dark-bright soliton train we study in this work occurs when one of the system's sound speeds becomes complex so that the standard definition of supersonic flow does not apply.

Our experiments are conducted with BECs confined in a single-beam optical dipole trap [9]. We start with an initially perfectly overlapped mixture of atoms in the  $|F, m_F\rangle = |1, 1\rangle$  and  $|2, 2\rangle$  hyperfine states of  $^{87}\text{Rb}$ , with a total of about 450000 atoms. The scattering lengths for the two states used in our experiment are estimated to be  $a_{11} = 100.40$  a.u. and  $a_{22} \approx a_{12} = 98.98$  a.u. [10]. Here  $a_{11}$  and  $a_{22}$  denote the single species scattering length for the  $|1, 1\rangle$  and  $|2, 2\rangle$  state, respectively, and  $a_{12}$  is the interspecies scattering length. Mean field theory predicts that a mixture is miscible if  $a_{12} < \sqrt{a_{11} \cdot a_{22}}$  [11–13]. Therefore our system is predicted to be weakly miscible. In contrast, previous studies of two-component binary  $^{87}\text{Rb}$  BECs concentrated mostly on the states which are immiscible [14, 15], with the notable exception of Weld et al. [16].

When the overlapped mixture is allowed to evolve in the trap, we observe no phase separation over the experimental timescale of several seconds. This is in agreement with the predicted miscibility of the two components and is demonstrated in Fig. 1(a-c). The upper cloud of each

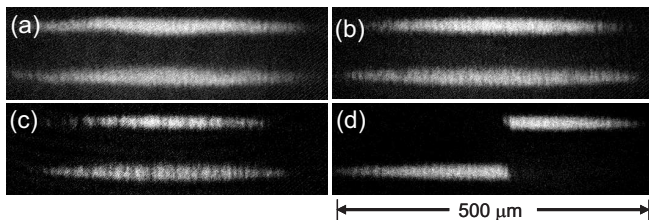


FIG. 1: Time evolution of an initial perfectly overlapped mixture without (a-c) and with (d) an applied axial magnetic gradient. Images taken after (a) 100 ms, (b) 1 sec and (c, d) 9 sec of in-trap evolution.

image throughout this work shows the atoms in the  $|2, 2\rangle$  state at a time 7 ms after a sudden turn-off of the optical trap (and, where applicable, of any applied magnetic gradients), while the lower cloud, taken during the same experimental run, shows the atoms in the  $|1, 1\rangle$  state after 8 ms of expansion [9]. During their in-trap evolution, these clouds are overlapped in the vertical direction. The dominant effect of the time evolution in Fig. 1(a-c) is a slow decay of the atom number over time. For single component BECs, we have measured an exponential BEC lifetime of over 50 sec for the  $|1, 1\rangle$  state and 14 sec for the  $|2, 2\rangle$  state in our dipole trap. Motion induced by changes of mean field pressure during the decay may be responsible for a small scale roughness of both components which becomes visible after several seconds (Fig. 1c).

The situation changes when a small magnetic gradient is applied along the long axis of the trap. Due to Zeeman shifts, the gradient leads to a force in opposite directions for each component, or equivalently to a differential shift between the harmonic potentials along the long axis of the trap. This causes the two components to accelerate in opposite directions and induces counterflow. In all images where a magnetic gradient is applied, the gradient is chosen such that the  $|2, 2\rangle$  state is pulled to the right and the  $|1, 1\rangle$  to the left. An example is shown in Fig. 1d where a gradient leading to a calculated differential trap shift of  $60 \mu\text{m}$  was applied for 9 sec, leading to nearly complete demixing of the two components.

In the following we investigate the dynamics induced by small gradients and show how they can be exploited to create dark-bright soliton trains. In Fig. 2 an initially overlapped mixture of 30% of the atoms in the  $|2, 2\rangle$  state and 70% in the  $|1, 1\rangle$  state is used. A small magnetic gradient in the axial direction is linearly ramped on over a timescale of 1 sec, leading to a calculated trap separation for the two species of only about three microns. After the end of this ramp, the gradient is held constant. In the subsequent evolution, individual stripes break off from the left edge of the  $|2, 2\rangle$  component, and perfectly aligned dark notches appear in the  $|1, 1\rangle$  component (Fig. 2(a)). The predominantly uniform widths of the observed stripes and notches, their long lifetime of several seconds in the absence of a magnetic gradient,

as well as their dynamics resembling individual stable entities (see Fig. 4 and below) are strong experimental indications that the observed features are indeed dark-bright solitons. By reducing the initial number of atoms in the component forming the bright soliton, we have also been able to reliably produce one individual dark-bright soliton and observe its oscillation in trap [17], similar to the dynamics observed in [6].

The observed soliton formation is reproduced by three-dimensional (3D) numerical simulations of the two-component Gross-Pitaevskii (GP) equations (Fig. 2(b-e)) [9]. Parameters used for the GP equations are the experimental values. These values lead to dynamics that closely match the experiment, as shown in Fig. 2(a-c) with a moderate time delay. Our numerical calculations suggest that the time delay may be due to uncertainties in the estimated magnetic field gradient induced trap shifts. The experimentally invoked free expansion directly before imaging the condensate was not performed in the numerical simulations.

Numerical results for the quantum mechanical phases of the two wavefunctions describing the components are shown in Fig. 2(e). The nearly linear phase behavior on the right (at  $x \gtrsim 50 \mu\text{m}$ ) indicates a smooth counterflow of the two components. In the soliton region, the phase jumps across the dark solitons as well as the phase gradients in the bright component vary slightly, so that the dark-bright solitons are moving relative to one another which eventually leads to dark-bright soliton interactions, see [9].

The soliton train formation can be qualitatively understood by appealing to the hydrodynamic formulation of the mean-field, coupled GP equations in (1+1) dimensions

$$\begin{aligned}
 (\rho_j)_t + (\rho_j u_j)_z &= 0 \\
 (u_j)_t + \left( \frac{1}{2} u_j^2 + \rho_j + \sigma_j \rho_{3-j} \right)_z &= \frac{1}{4} \left[ \frac{(\rho_j)_{zz}}{\rho_j} - \frac{(\rho_j)_z^2}{2\rho_j^2} \right],
 \end{aligned} \tag{1}$$

here given in non-dimensional form with  $\sigma_j = a_{12}/a_{jj}$ ,  $\rho_j$  and  $u_j$ ,  $j = 1, 2$  the density and phase gradient (superfluid velocity) of the  $j^{\text{th}}$  component, respectively. Equation (1) models the dynamics of a highly elongated cigar shaped trap ( $\omega_x \sim \omega_y \gg \omega_z$  where  $\omega_x$  ( $\omega_y$ ) is the transverse trap frequency in the horizontal (vertical) plane and  $\omega_z$  is the axial trap frequency) with axial confinement neglected [1]. Distance is in units of the transverse harmonic oscillator length  $\sqrt{\hbar/(m\omega_x)}$  ( $m$  is the particle mass). Time is in units of  $1/\omega_x$  and the 3D densities are approximated by the harmonic oscillator ground state via  $\rho_j(z, t) \exp(-x^2 - \frac{\omega_y}{\omega_x} y^2)/(2\pi a_{jj} a_0^2)$ .

By considering small perturbations proportional to  $e^{i(\kappa z - \omega t)}$  for uniform counterflow with densities  $\rho_j$  and velocities  $u_1 = -v/2$ ,  $u_2 = v/2$ , Ref. [3] demonstrated modulational instability ( $\text{Im } \omega(\kappa) > 0$ ) for  $v$  larger than a critical velocity  $v_{\text{cr}}$  with a maximum growth rate  $\text{Im } \omega_{\text{max}}$

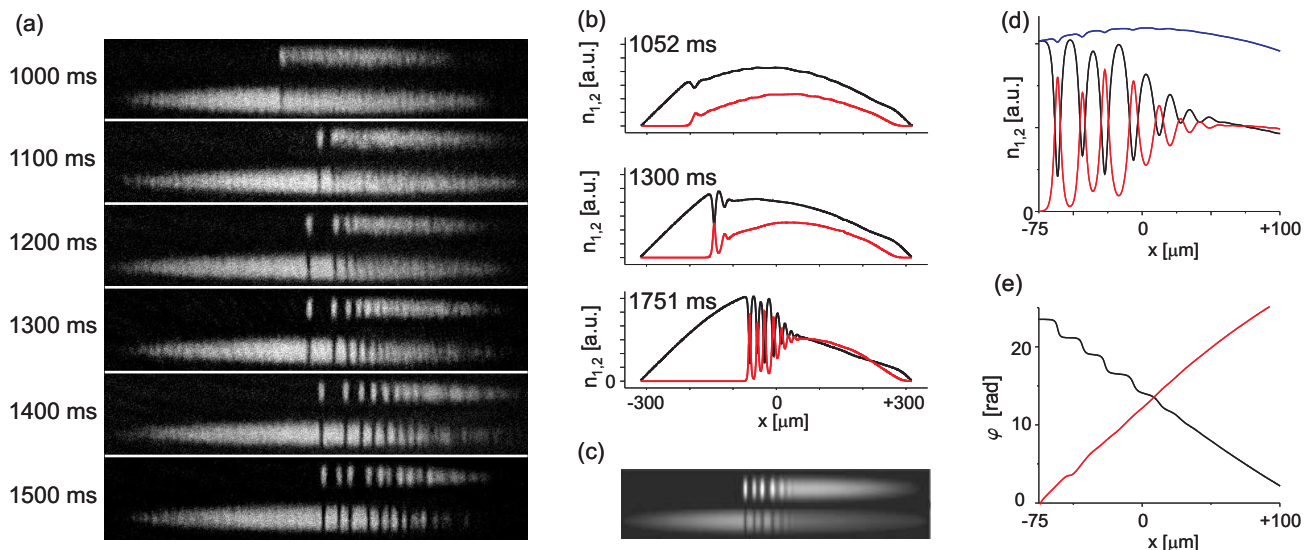


FIG. 2: Formation of dark-bright soliton trains during superfluid-superfluid counterflow. A mixture with 70% of all atoms in the  $|1, 1\rangle$  state (lower cloud in (a) and (c); black line in (b),(d),(e)) and 30% in the  $|2, 2\rangle$  state (upper cloud and red lines, resp.) is created. An axial gradient is ramped on over 1 sec and held constant thereafter. (a) Experimental images of soliton train formation. Times are measured from start of ramp. (b) Integrated cross sections of 3D numerical simulations, revealing a gradually steepening overlap interface and subsequent soliton formation. (c) Integrated density plot of 3D numerics at 1751 ms. Field of view  $627 \mu\text{m} \times 17 \mu\text{m}$ . (d) Zoomed-in view of soliton train in (b) at 1751 ms. The blue line shows the total density. (e) Phase behavior for region shown in (d).

and associated wavenumber  $\kappa_{\text{max}}$ . We have repeated the calculation and find the additional result

$$\sqrt{\rho_1(1 - \sigma_1\sigma_2)} \leq v_{\text{cr}} \leq 2\sqrt{\rho_1(1 - \sqrt{\sigma_1\sigma_2})}, \quad \rho_1 \geq \rho_2, \quad (2)$$

the lower bound being valid for small  $\rho_2/\rho_1$  and the upper bound applicable for  $\rho_2 \sim \rho_1$ . The scattering lengths of the binary system considered here give  $0.119\sqrt{\rho_1} \leq v_{\text{cr}} \leq 0.168\sqrt{\rho_1}$ . Typical densities for the experiments in Fig. 2 give  $\rho_1 + \rho_2 = 4.3$ ,  $\rho_2/\rho_1 = 0.3$  leading to  $v_{\text{cr}} = 0.25$  ( $\approx 0.22 \text{ mm/s}$ ).

Figure 2 shows that the dark-bright soliton train forms at the overlap interface of the two components while approximately maintaining constant total density. We model this by numerically solving eq. (1) for an initial jump in density that maintains  $\rho_1 + \rho_2 = 4.3$  (dotted curves in 3(a,b)) with a uniform counterflow:  $u_1 = -v/2$  and  $u_2 = v/2$ . For subcritical cases  $0 \leq v < v_{\text{cr}}$ , the evolution consists of an expanding rarefaction wave with weak oscillations on the right edge (Fig. 3(a); solid line for  $v = 0$ , dashed line for  $v = 0.17$ ) and corresponding scaled relative speeds  $|u_1 - u_2|/\sqrt{\rho_1}$  (Fig. 3(c) solid, dashed) below critical (in Fig. 3(c,d), the bounds (2) on the critical velocities are indicated by the dotted lines). When the initial relative speed is supercritical, a dark-bright soliton train forms at the initial jump (Fig. 3(b),  $v = 0.32$ ). The relative speed within some regions of the soliton train significantly exceeds  $v_{\text{cr}}$  as shown in Fig. 3(d) suggesting that counterflow induced MI has the effect of enhancing soliton formation. Because the initial

relative speed  $v$  was taken just slightly above  $v_{\text{cr}}$ , the maximum growth rate  $\text{Im}\omega_{\text{max}} = 0.0077$  and associated wavenumber  $\kappa_{\text{max}} = 0.13$  for unstable perturbations to the uniform state in the far field are small (Figs. 3(e,f)). Therefore, MI in the background counterflow far from the jump does not develop appreciable magnitude over the timescale of soliton train formation, in contrast to the dynamics with  $v \gg v_{\text{cr}}$  that we investigate in [18].

This MI assisted soliton formation technique allows us to create dark-bright solitons in a well-controlled and repeatable manner, as is evidenced by the fact that all images of Fig. 2a form a very consistent sequence even though they were taken during different runs of the experiment. In addition to repeatability, future studies may also require a long lifetime of the solitons. In single component BECs, achieving long lifetimes of dark solitons has proven difficult as they are subject to a transverse instability [5, 8]. Only recently have dark soliton lifetimes of up to 2.8 sec been achieved [6]. It has been conjectured [19] and numerically confirmed [20] that dark-bright solitons are more stable to transverse perturbations than dark solitons. Experimentally, we indeed observe long lifetimes of several seconds for the dark-bright solitons after the magnetic gradient is turned off. The solitons act as individual entities and can move through the BEC, maintaining their shape for a relatively long time. We demonstrate this by starting from a situation as in Fig. 2(a) at 1.5 sec, where a train of solitons has been created after the application of an axial magnetic gradient. When the gradient is subsequently turned off,

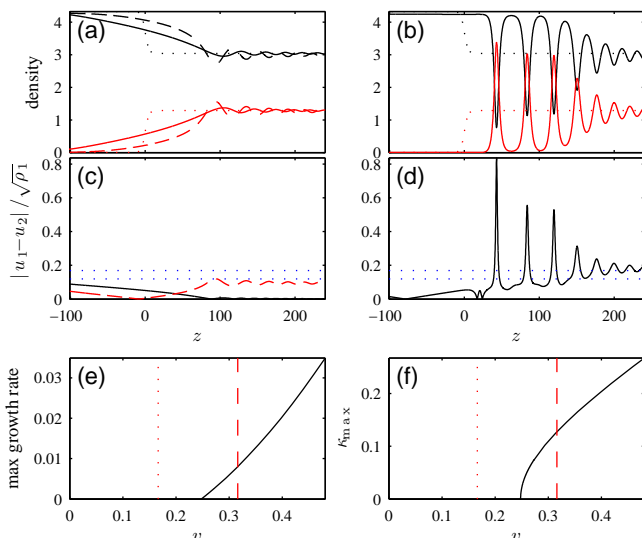


FIG. 3: densities (a,b) and relative speeds (c,d) at  $t = 462$ . (e,f): maximum growth rate and associated wavenumber of unstable perturbations. Vertical lines correspond to subcritical (dotted) and supercritical (dashed) cases of (a-d). See text for further details.

the dark-bright solitons move through the BEC while approximately maintaining their narrow widths (Fig. 4). The bright and dark part of each individual soliton remain aligned relative to each other, but any regularity in the spacing between solitons is lost. The number of visible solitons decreases over time, but even after 2.5 sec several solitons are still visible, as in Fig. 4(d). Simulations [9] suggest that soliton interactions may be the cause of this decay. In Fig. 4(c), little diffuse cloudlets of atoms in the  $|2, 2\rangle$  state are visible in addition to some solitons, and corresponding small suppressions of the density in the  $|1, 1\rangle$  components can be detected. We interpret these features as the decay products of dark-bright solitons, marking the end of their life cycle.

In conclusion, we have observed dark-bright soliton trains in the counterflow of two miscible superfluids. The soliton train is formed due to relative motion above the critical value for modulational instability. By inducing relative speeds slightly above critical, we can avoid the onset of MI throughout the superfluids over the time scales of soliton train formation. Together with the long lifetime of the observed dark-bright solitons, this opens the door to future experiments with these interesting coherent nonlinear structures. While the dynamics considered in this Letter are effectively one-dimensional, a very recent theoretical analysis has shown that superfluid counterflow in higher dimensions can lead to binary quantum turbulence, providing another example of the exceptional dynamical richness of the two-component system [21].

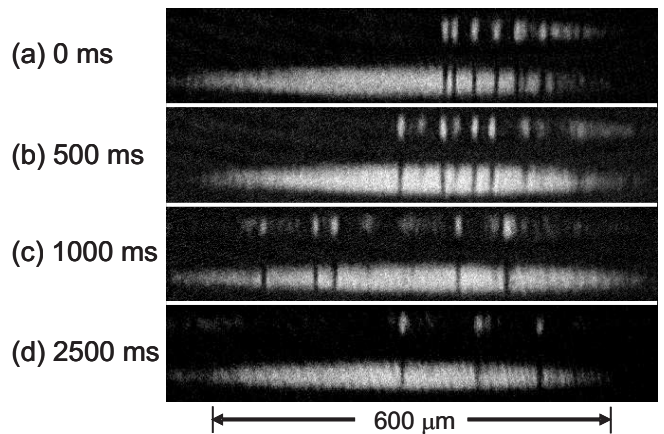


FIG. 4: Motion of dark-bright solitons. After creating dark-bright solitons as in Fig. 2(a), the axial magnetic gradient is removed and the mixture is allowed to evolve in trap for the evolution times given next to each image. The solitons spread out through the mixture.

### Acknowledgments

P.E. acknowledges financial support from NSF and ARO. M.A.H. acknowledges financial support from NSF under DMS-0803074, DMS-1008973 and a Faculty Research and Professional Development grant from NCSU. The authors thank the anonymous referees for beneficial suggestions.

\* Electronic address: engels@wsu.edu

- [1] P. G. Kevrekidis, D. Frantzeskakis, and R. Carretero-Gonzalez, *Emergent Nonlinear Phenomena in Bose-Einstein Condensates: Theory and Experiment* (Springer, Berlin Heidelberg, 2009).
- [2] See, e.g., R. J. Donnelly, *Quantized vortices in helium II* (Cambridge University Press, Cambridge, 1991).
- [3] C. K. Law *et al.*, Phys. Rev. A **63**, 063612 (2001).
- [4] V. Zakharov and L. Ostrovsky, Physica D **238**, 540 (2009).
- [5] B. Anderson *et al.*, Phys. Rev. Lett. **86**, 2926 (2001).
- [6] C. Becker *et al.*, Nature Physics **4**, 496 (2008).
- [7] A. M. Kamchatnov *et al.*, Phys. Lett. A **319**, 406 (2003).
- [8] Z. Dutton, *et al.*, Science **293** 663 (2001). A. M. Kamchatnov, A. Gammal, and R. A. Kraenkel, Phys. Rev. A, **69**, 063605 (2004). M. A. Hofer *et al.*, Phys. Rev. A **74**, 023623 (2006). R. Meppelink *et al.*, Phys. Rev. A, **80**, 043606 (2009).
- [9] See EPAPS for experimental and numerical details, as well as a movie of the numerical simulations. For more information on EPAPS, see <http://www.aip.org/pubservs/epaps.html>.
- [10] B. J. Verhaar, E. G. M. van Kempen, and S. J. J. M. F. Kokkelmans, Phys. Rev. A **79**, 032711 (2009). S. J. J. M. F. Kokkelmans, personal communication, (2010).

- [11] E. Timmermans, Phys. Rev. Lett. **81**, 5718 (1998).
- [12] P. Ao and S. T. Chui, Phys. Rev. A **58**, 4836 (1998).
- [13] H. Pu and N. P. Bigelow, Phys. Rev. Lett. **80**, 1130 (1998).
- [14] D. S. Hall *et al.*, Phys. Rev. Lett. **81**, 1539 (1998).
- [15] K. M. Mertes *et al.*, Phys. Rev. Lett **99**, 190402 (2007).
- [16] D. M. Weld *et al.*, Phys. Rev. Lett. **103**, 245301 (2009).
- [17] S. Middelkamp *et al.*, Physics Letters A (2010), doi:10.1016/j.physleta.2010.11.025.
- [18] M. A. Hoefer *et al.*, arXiv:1007.4947 [cond-mat.quant-gas].
- [19] T. Busch and J. R. Anglin, Phys. Rev. Lett. **87**, 010401 (2001).
- [20] Z. H. Musslimani and J. Yang, Optics Letters **26**, 1981 (2001).
- [21] H. Takeuchi, S. Ishino, and M. Tsubota, Phys. Rev. Lett. **105**, 205301 (2010).